

## Spreading Widths of Isoscalar Giant Quadrupole Resonances in $^{16}\text{O}$ and $^{40}\text{Ca}$

T. Hoshino and A. Arima

*Department of Physics, University of Tokyo, Tokyo 113, Japan*

(Received 10 November 1975)

Isoscalar giant quadrupole resonances are theoretically studied for  $^{16}\text{O}$  and  $^{40}\text{Ca}$ . A remarkable difference in the widths of these resonances observed in  $(\alpha, \alpha')$  experiments is explained. Both one-particle, one-hole and two-particle, two-hole correlations are found to be responsible for producing the difference.

Many experiments on the isoscalar giant quadrupole resonances (GQR) have been published.<sup>1</sup> Recent  $(\alpha, \alpha')$  experiments have revealed that the width of the GQR below  $A = 40$  systematically broadens as the mass number decreases;  $3.5 \pm 0.3$  in  $^{40}\text{Ca}$ ,  $7.1 \pm 0.5$  in  $^{32}\text{S}$ ,<sup>2</sup> and  $7.5 \pm 1$  in  $^{16}\text{O}$  (full width at half-maximum in MeV).<sup>3</sup> It also should be noted that the shape of the GQR in  $^{16}\text{O}$  is very different from the approximate Gaussian peak observed in medium and heavy nuclei.<sup>3,4</sup>

The simplest picture to describe the GQR assumes a coherent mixture of one-particle, one-hole (1p-1h) states which are frequently approximated to be bound states with  $2\hbar\omega$  excitation in the harmonic-oscillator shell model.<sup>5</sup> This picture can explain reasonably well the observed excitation energies. Two kinds of couplings of the coherent state with states other than the 1p-1h states must be taken into account. One is coupling with continuum states,<sup>6,7</sup> which gives rise to escaping widths. The theoretical escaping widths<sup>7</sup> are about 0.5 MeV for  $^{40}\text{Ca}$  and 1.2 MeV for  $^{16}\text{O}$ , which are much smaller than the observed widths. The other is coupling with 2p-2h states which causes spreading widths. This coupling must be important, because many 2p-2h states have the same zeroth-order energy of  $2\hbar\omega$  as the 1p-1h GQR.

In order to show the importance of the spreading width, we have performed a shell-model calculation for the GQR in  $^{16}\text{O}$  and  $^{40}\text{Ca}$ . All  $T=0$   $2\hbar\omega$  excited states are taken into account to describe the GQR, while the ground states are assumed to have  $0\hbar\omega$  closed-shell configurations. Spurious states with excitations of center-of-mass motion must be eliminated from the model space. Because these consist mainly of the 2p-2h states, the 1p-1h components are still dominant in the states, hereafter called "1p-1h" states, obtained by eliminating the spurious states from the 1p-1h states and further orthogonalizing the remainder. Other states which are orthogonal to the "1p-1h" and spurious states

consist only of the 2p-2h states. One can thus decompose the nonspurious  $2\hbar\omega$  space into the "1p-1h" and nonspurious 2p-2h subspaces.

A model Hamiltonian is assumed to consist of a single-particle Hamiltonian and a two-body residual interaction. As the residual interaction we assumed a phenomenological central potential of Gaussian form with the Rosenfeld exchange mixture:

$$V(r) = -V_0(-0.33P_{33} + 0.6P_{31} + P_{13} - 1.8P_{11}) \times \exp[-(r/r_0)^2]. \quad (1)$$

The range parameter  $\lambda = r_0/\sqrt{2}b$  (where  $b$  is the oscillator length parameter) is taken to be 0.71 for  $^{16}\text{O}$  and 0.66 for  $^{40}\text{Ca}$ . ( $b = 1.85$  fm for  $^{16}\text{O}$  and  $b = 2.00$  fm for  $^{40}\text{Ca}$ .) The depth parameter  $V_0$  is assumed to be 50 MeV for  $^{16}\text{O}$  and 45 MeV for  $^{40}\text{Ca}$ . The present value for  $^{16}\text{O}$  reproduces approximately the excitation energy of the level at 11.52 MeV, which is suggested to be the lowest 2p-2h state by the  $^{14}\text{N}(\alpha, d)$  experiment<sup>8</sup> (see Table II). The above value of  $V_0$  for  $^{40}\text{Ca}$  is standard in the shell-model calculations in the  $A = 40$  region. The single-particle energies are shown in Table I.

Before the full  $2\hbar\omega$  calculation, we diagonalize the Hamiltonian in the "1p-1h" subspace. The calculation gives a state which exhausts more than 92% of the theoretical limit on the total sum of the isoscalar  $B(E2)$  strength from the 0p-0h state. For this state, hereafter called the "1p-1h" GQR, the calculation gives the following  $B(E2)$  values and excitation energies:  $B(E2) = 93e^2 \text{ fm}^4$  (92.7%) and  $E_x = 23.3$  MeV for  $^{16}\text{O}$ , and  $B(E2) = 460e^2 \text{ fm}^4$  (97.6%) and  $E_x = 18.4$  MeV for  $^{40}\text{Ca}$ . The percentages in the parentheses are the  $B(E2)$  values relative to the theoretical limit values. These results are consistent with those of other calculations.<sup>6,7</sup>

The results of the full  $2\hbar\omega$  calculation together with experimental data are shown in Table II and Fig. 1. The calculated  $B(E2)$  for  $^{16}\text{O}$  is now spread over a wide range of energy and shows

TABLE I. Single-particle energies of neutrons (in MeV) used in the calculation, which were determined in Ref. 9 for  $^{16}\text{O}$  and in Ref. 10 for  $^{40}\text{Ca}$  from experiments, except for those noted.

$nl$	$j$	$^{16}\text{O}$		$^{40}\text{Ca}$	
		$l+1/2$	$l-1/2$	$l+1/2$	$l-1/2$
0s		-48.00			
0p		-21.74	-15.60	-43.00 <sup>a</sup>	-40.00 <sup>a</sup>
0d		-4.15	0.93	-21.25	-15.64
1s		-3.28		-18.11	
0f		15.00	22.00	-8.36	-2.86
1p		20.00	23.00	-6.29	-4.23
0g				8.00 <sup>b</sup>	17.00 <sup>b</sup>
1d				10.00 <sup>b</sup>	15.00 <sup>b</sup>
2s				12.00 <sup>b</sup>	

<sup>a</sup>Determined from an  $(e, e'p)$  experiment with the Coulomb energy correction.

<sup>b</sup>Adjusted to reproduce the excitation energy of the GQR. A constant  $l$ - $s$  splitting is assumed.

no prominent peaks of Gaussian or Lorentzian shape, which is very consistent with the  $(\alpha, \alpha')$  data.<sup>3,4</sup> The shape of the total  $E2$  photoabsorption cross section is calculated from the calculated  $B(E2)$  by using the expression

$$\sigma_{E2} = [3(2\pi E_\gamma)^3 / 50(e\hbar c)^2] B(E2) \delta(E_\gamma - E_x), \quad (2)$$

where  $E_\gamma$  is the energy of the photon. The shape is in reasonable agreement with that of the observed  $(\gamma, p_0)$  cross section deduced from the  $(p_{\text{pol}}, \gamma_0)$  data<sup>12</sup> using detailed balance. The calculated absolute strength is consistent with the data in view of the possible contribution of other channels, which is, however, not estimated in any available theoretical papers. The  $E2$  strengths for lower levels predicted by the present calculation are much too small compared with the observed values. This is not totally unexpected, because the present calculation neglects the deformed and/or many-particle, many-hole components, and the ground-state correlation.

For  $^{40}\text{Ca}$ , the full  $2\hbar\omega$  calculation spreads the "1p-1h" GQR very little. There appears a prominent peak with a narrow width in contrast to  $^{16}\text{O}$ . This is in good agreement with the  $(\alpha, \alpha')$  data.<sup>2,13</sup> The width and total strength observed in the  $(e, e')$  experiment<sup>14</sup> are apparently twice as large as the relevant values obtained from the  $(\alpha, \alpha')$  data. One should, however, remember that the spin and parity of the whole resonance are assumed to be  $2^+$  in the analysis of the  $(e, e')$  data. The upper half of the resonance seems to coincide with the

TABLE II. Calculated isoscalar and experimental  $E2$  strengths  $S$  in the percentage of the energy-weighted sum rule (EWSR) limit value for isoscalar  $E2$  transition.

	$^{16}\text{O}$		$^{40}\text{Ca}$	
	Ex (MeV)	S (%)	Ex (MeV)	S (%)
Calculation				
	20~30	87.8	14~22	77.9
	10~20	2.9	7~14	1.6
	(19~28)	81.6		
lowest 2p-2h	10.50	1.15	7.60	0.15
Experiment				
	15.9~27.3	58±25 <sup>a</sup>	17.9	44±10 <sup>e</sup>
	18.4	9	( $\Gamma=3.5\pm0.3$ )	
	6.92~13.1	25		
$(\alpha, \alpha')$	20.1~24.4	31.3 <sup>b</sup>	18.25	32 <sup>f</sup>
	18.0~19.5	13.8	(16~21)	
	6.92~15.2	22.3		
	20~30	21±8 <sup>c</sup>	10~22	66 <sup>g</sup>
$(e, e')$	18.5	4	(16~22)	37 <sup>h</sup>
	6.92~13.1	39		
$(p, \gamma_0)$	24 (19~28)	55 <sup>d</sup>		
lowest 2p-2h	11.52	12.2±1.3 <sup>c</sup>	6.91	5.5±1.5 <sup>h</sup>

<sup>a</sup>Ref. 3. The  $S$  value from  $E_x = 15.9$  to 27.3 MeV does not include the strengths of the 18.4-MeV group.

<sup>b</sup>Ref. 4.

<sup>c</sup>Ref. 11.

<sup>d</sup>Ref. 12; the EWSR-limit value is corrected to the present value from that used in the original paper.

<sup>e</sup>Ref. 2.

<sup>f</sup>Ref. 13.

<sup>g</sup>Ref. 14.

<sup>h</sup>Ref. 15. The present EWSR-limit values [ $2420 e^2 \text{ fm}^4 \text{ MeV}$  for  $^{16}\text{O}$  and  $9830 e^2 \text{ cm}^4 \text{ MeV}$  for  $^{40}\text{Ca}$ ] are deduced from observed rms charge radii.

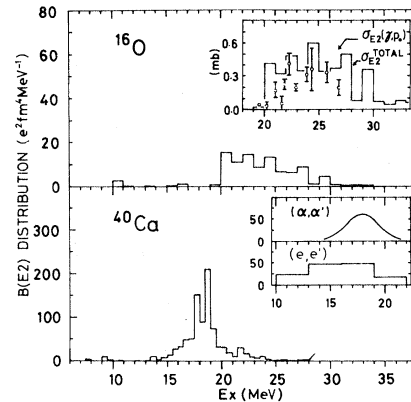


FIG. 1. Calculated distributions of isoscalar  $B(E2)$  ( $g.s. \rightarrow J^\pi T = 2^+ 0$ ). The inset for  $^{16}\text{O}$  provides the calculated total  $E2$  photoabsorption cross section (solid line) and experimental  $(\gamma, p_0)$  cross section (circles) deduced from Ref. 12. That for  $^{40}\text{Ca}$  provides the experimental distribution observed in the  $(\alpha, \alpha')$  (Ref. 2) and the  $(e, e')$  (Ref. 14) reactions. The calculation for  $^{40}\text{Ca}$  is restricted to  $E_x \leq 28$  MeV.

GQR observed in the composite-nuclear-particle scattering experiments, but the lower half could be a giant resonance of another multipolarity, possibly  $E0$ .<sup>16</sup>

The classical formula for the spreading width  $\Gamma^\dagger$  is given by<sup>17</sup>

$$\Gamma^\dagger = 2\pi V^2/D, \quad (3)$$

where  $V$  is the coupling matrix element between the relevant doorway state and compound states which are spaced with a distance  $D$ . This formula holds under the condition that  $V$  and  $D$  are constant. Associating the doorway (compound) state(s) with the "1p-1h" GQR (2p-2h states) obtained by the diagonalization of the Hamiltonian in the "1p-1h" (2p-2h) subspace, we analyze the corresponding  $V$  which will hereafter be denoted by  $V_i(i)$  for the  $i$ th 2p-2h state.

The following correlations are expected to affect the spreading width: (a) 1p-1h correlation, and (b) 2p-2h correlation. The first is responsible for producing the "1p-1h" GQR. Using a very schematic model, Bertsch<sup>18</sup> first and then U<sup>19</sup> pointed out that this correlation turns out to weaken the coupling of the "1p-1h" GQR with the 2p-2h states making the  $\Gamma^\dagger$  of the GQR much smaller than that of a particle or a hole state. According to their theory  $\Gamma^\dagger$  is zero, because of complete cancellation of  $V_p(i)$  by  $V_h(i)$  for any 2p-2h state irrespective of the 2p-2h correlation:

$$V_i(i) \equiv V_p(i) + V_h(i) = 0, \quad (4)$$

$$V_p(i) \equiv \langle 1p-1h; \text{GQR} | H_{1p,2p-1h} | 2p-2h; i \rangle, \quad (5)$$

$$V_h(i) \equiv \langle 1p-1h; \text{GQR} | H_{1h,1p-2h} | 2p-2h; i \rangle, \quad (6)$$

where  $H_{1p,2p-1h}$  ( $H_{1h,1p-2h}$ ) stands for an interaction Hamiltonian between one-particle (one-hole) and two-particle, one-hole (one-particle, two-hole) states. The present calculation with use of more realistic interaction, however, showed that the cancellation is not complete for the two nuclei, particularly for  $^{16}\text{O}$ . By comparing the  $V_i^2$  density and the  $V_p^2 + V_h^2$  density, one can see more clearly how much the cancellation occurs in the present cases. Figure 2 shows that the cancellation effect is very weak in  $^{16}\text{O}$ , whereas it is rather important in  $^{40}\text{Ca}$ .

Because the cancellation is not complete, the 2p-2h correlation must be taken into account to understand the mechanism of the spreading width. Without this correlation, the  $V_i^2$  density is proportional to the level density  $\rho$  of the 2p-2h states. The 2p-2h correlation, however, makes certain 2p-2h states couple strongly with the "1p-1h"

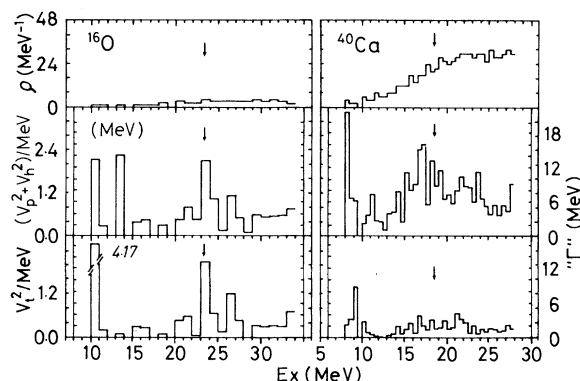


FIG. 2. Top: the distribution of the level density  $\rho$ . Middle: the distribution of the  $V_p^2 + V_h^2$  density. Bottom: the distribution of the  $V_i^2$  density. " $\Gamma$ " on the right-hand side denotes  $2\pi$  times  $V_p^2 + V_h^2$  or  $V_i^2$  density; the measure is indicated on the inner Y axis. [See Eq. (3) and relevant explanations in the text.] The arrows are located at the excitation energies of the "1p-1h" GQR's.

GQR. In  $^{16}\text{O}$ , such 2p-2h states appear in the vicinity of the "1p-1h" GQR and the condition of constant  $V$  in Eq. (3) is badly violated (see Fig. 2). Therefore the spreading width becomes large and the shape of the GQR deviates much from the Lorentzian.

Even in  $^{40}\text{Ca}$ , the 2p-2h correlation makes the distribution of  $V_i^2$  considerably different from that of the 2p-2h states. The  $V_i^2$  density, which corresponds to  $V^2/D$  in Eq. (3), is much flatter in  $^{40}\text{Ca}$  than in  $^{16}\text{O}$ . This makes Eq. (3) approximately applicable for  $^{40}\text{Ca}$ .

The results of the above analysis are summarized as follows: (1) The drastic spreading of the GQR in  $^{16}\text{O}$  is produced by the strong 2p-2h correlation. The 1p-1h correlation, on the other hand, is weak here. (2) The 1p-1h correlation is strong in  $^{40}\text{Ca}$ . This correlation is responsible for the reduction of the width of the GQR in  $^{40}\text{Ca}$ . The fact that the 2p-2h correlation is much weaker in  $^{40}\text{Ca}$  than in  $^{16}\text{O}$  explains why the calculated distribution of  $B(E2)$  is nearly Lorentzian.

<sup>1</sup>S. S. Hanna, in *Proceedings of the International Conference on Nuclear Structure and Spectroscopy, Amsterdam, The Netherlands, 1974*, edited by H. P. Blok and A. E. Dieperink (Scholar's Press, Amsterdam, 1974), Vol. 2, p. 249, and references therein.

<sup>2</sup>D. H. Youngblood *et al.*, Phys. Rev. Lett. **34**, 748 (1975).

- <sup>3</sup>K. T. Knöpfle *et al.*, Phys. Rev. Lett. **35**, 779 (1975).  
<sup>4</sup>M. J. A. de Voigt *et al.*, in *Proceedings of the International Symposium on Highly Excited States in Nuclei, Jülich, Federal Republic of Germany, 1975*, edited by A. Faessler, C. Mayer-Boericke, and P. Turek (Kernforschungsanlage Jülich, GmbH, Federal Republic of Germany, 1975), Vol. 1, p. 5, and private communication.  
<sup>5</sup>For example, T. T. S. Kuo and E. Osnes, Nucl. Phys. **A226**, 204 (1974).  
<sup>6</sup>S. Shlomo and G. Bertsch, Nucl. Phys. **A243**, 507 (1975).  
<sup>7</sup>S. Krewald *et al.*, Phys. Rev. Lett. **33**, 1386 (1974).  
<sup>8</sup>M. S. Zisman, E. A. McClatchie, and B. G. Harvey, Phys. Rev. C **2**, 1271 (1970).  
<sup>9</sup>H. P. Jolly, Jr., Phys. Lett. **5**, 289 (1963).  
<sup>10</sup>C. K. Scott, Ph.D. thesis, McGill University, 1968 (unpublished).  
<sup>11</sup>A. Hotta *et al.*, Phys. Rev. Lett. **33**, 790 (1974).  
<sup>12</sup>S. S. Hanna *et al.*, Phys. Rev. Lett. **32**, 114 (1974).  
<sup>13</sup>L. L. Rutledge, Jr., and J. C. Hiebert, Phys. Rev. Lett. **32**, 551 (1974).  
<sup>14</sup>Y. Torizuka *et al.*, Phys. Rev. C **11**, 1174 (1975).  
<sup>15</sup>J. R. MacDonald *et al.*, Phys. Rev. C **3**, 219 (1971).  
<sup>16</sup>G. R. Hammerstein *et al.*, Phys. Lett. **49B**, 235 (1974).  
<sup>17</sup>A. Bohr and B. Mottelson, *Nuclear Structure* (North-Holland, Amsterdam, 1968), Vol. 1, p. 302.  
<sup>18</sup>G. Bertsch, Phys. Lett. **37B**, 470 (1971).  
<sup>19</sup>H. Ui, in *Proceedings of the Kawatabi Conference on New Giant Resonances*, Sendai, Japan, June 1975 (to be published), p. 105.

## Deuteron Form Factor and the Short-Distance Behavior of the Nuclear Force\*

Stanley J. Brodsky

*Stanford Linear Accelerator Center, Stanford University, Stanford, California 94305*

and

Benson T. Chertok

*American University, Washington, D. C. 20016*

(Received 24 May 1976)

The large- $q^2$  falloff of the elastic deuteron form factor is used to relate meson exchange to underlying quark currents, to relate the deuteron form factor to large-angle  $n$ - $p$  scattering, to demonstrate scale-invariant behavior of the nucleon-nucleon potential, and to determine the deuteron wave function at small  $n$ - $p$  separation.

In this Letter we present several new results and predictions on the connection between nuclear and particle physics which follow from a study of the implications of the deuteron having an underlying six-quark constituent structure.<sup>1,2</sup>

The deuteron form factor  $F_D(q^2)$  provides an ideal illustration of the continuity between nuclear and particle physics at the microscopic level. At low momentum transfers, where the nucleons can be treated as pointlike objects and are the essential degrees of freedom, the usual effective-potential Schrödinger theory is appropriate, and meson-exchange effects provide the framework for the nuclear interaction. However, at large momentum transfers where the nucleon form factor differs significantly from its  $-q^2 = 0$  value, hadronic substructure comes into play and the electromagnetic interaction begins to resolve an elementary fermion current. The quark degrees of freedom then become appropriate. The elastic form factor of the nucleus is equivalent to the probability amplitude to rearrange  $n$  elementary

constituents; the dimensional counting prediction,

$$(q^2)^{n-1} F_n \rightarrow \text{const}, \quad (1)$$

then follows assuming a scale-invariant theory.<sup>2</sup> The power law in Eq. (1) is to be contrasted with bootstrap or continuum models with a uniform current distribution. These theories imply an infinitely composite hadronic structure and exponentially damped form factors. Experiment appears to be consistent with Eq. (1) for the pion ( $n=2$ ) and the proton ( $n=3$ ) for  $q^2 \gg M^2$ . The pion form-factor data extend from 9 GeV<sup>2</sup> in the timelike region ( $q^2 > 0$ ) to -4 GeV<sup>2</sup> in the spacelike region and the proton data extend to -33 GeV<sup>2</sup>. The recent measurement<sup>1</sup> of the deuteron elastic form factor out to  $-q^2 = 6$  GeV<sup>2</sup> appears to be consistent with an underlying six-quark structure for this elementary nucleus.

The deuteron form factor has been investigated using the simplest quark diagrams, in particular a democratic-chain model and a constituent-interchange model. These models are constrained